



ELSEVIER

Contents lists available at ScienceDirect

Developmental Biology

journal homepage: www.elsevier.com/locate/developmentalbiology

Peroxisomal membrane channel Pxmp2 in the mammary fat pad is essential for stromal lipid homeostasis and for development of mammary gland epithelium in mice



Miia H. Vapola^a, Aare Rokka^a, Raija T. Sormunen^b, Leena Alhonen^c, Werner Schmitz^d, Ernst Conzelmann^d, Anni Wärrä^e, Silke Grunau^a, Vasily D. Antonenkov^{a,*}, J. Kalervo Hiltunen^{a,*}

^a Faculty of Biochemistry and Molecular Medicine and Biocenter Oulu, University of Oulu, P.O. Box 3000, FI-90014 Oulu, Finland

^b Department of Pathology and Biocenter Oulu, University of Oulu, FI-90014 Oulu, Finland

^c A.I. Virtanen Institute for Molecular Sciences, University of Kuopio, FI-70211 Kuopio, Finland

^d Theodor-Boveri-Institut für Biowissenschaften (Biocentrum) der Universität Würzburg, D-97074 Würzburg, Germany

^e Georgetown University Medical Center, Department of Oncology, Washington, DC 20057, USA

ARTICLE INFO

Article history:

Received 25 June 2013

Received in revised form

25 March 2014

Accepted 26 March 2014

Available online 12 April 2014

Keywords:

Pxmp2

Peroxisomes

Membrane channels

Lipid metabolism

Mammary glands

ABSTRACT

To understand the functional role of the peroxisomal membrane channel Pxmp2, mice with a targeted disruption of the *Pxmp2* gene were generated. These mice were viable, grew and bred normally. However, *Pxmp2*^{-/-} female mice were unable to nurse their pups. Lactating mammary gland epithelium displayed secretory lipid droplets and milk proteins, but the size of the ductal system was greatly reduced. Examination of mammary gland development revealed that retarded mammary ductal outgrowth was due to reduced proliferation of epithelial cells during puberty. Transplantation experiments established the *Pxmp2*^{-/-} mammary stroma as a tissue responsible for suppression of epithelial growth. Morphological and biochemical examination confirmed the presence of peroxisomes in the mammary fat pad adipocytes, and functional Pxmp2 was detected in the stroma of wild-type mammary glands. Deletion of Pxmp2 led to an elevation in the expression of peroxisomal proteins in the mammary fat pad but not in liver or kidney of transgenic mice. Lipidomics of *Pxmp2*^{-/-} mammary fat pad showed a decrease in the content of myristic acid (C₁₄), a principal substrate for protein myristoylation and a potential peroxisomal β-oxidation product. Analysis of complex lipids revealed a reduced concentration of a variety of diacylglycerols and phospholipids containing mostly polyunsaturated fatty acids that may be caused by activation of lipid peroxidation. However, an antioxidant-containing diet did not stimulate mammary epithelial proliferation in *Pxmp2*^{-/-} mice.

The results point to disturbances of lipid metabolism in the mammary fat pad that in turn may result in abnormal epithelial growth. The work reveals impaired mammary gland development as a new category of peroxisomal disorders.

© 2014 Elsevier Inc. All rights reserved.

Introduction

An emerging link between breast carcinogenesis and abnormalities in the growth of mammary glands during puberty and

pregnancy underlines the importance of identifying mechanisms governing development of this organ (Lanigan et al., 2007; McCready et al., 2010). The mouse mammary gland is a useful model for investigating these mechanisms (Howlin et al., 2006; Brisken, 2013) since, like the human gland, it consists of ductal and alveolar epithelium embedded in mammary stroma. However, composition of the stroma shows some differences. It consists of the homogeneous adipose tissue in the mouse while the human stroma is more enriched by highly vascularized connective tissue (Hovey and Aimò, 2010). In both human and mouse epithelial growth comprises ductal elongation, side branching, and development of alveoli (McNally and Martin, 2011). Enhanced epithelial

Abbreviations: DAB, 3,3'-diaminobenzidine tetrahydrochloride; ERα, estrogen receptor α; PPAR, peroxisome proliferator-activated receptor; TEB, terminal end buds; VLCFA, very long chain fatty acids; WAP, whey acidic protein; TBA-RS, thiobarbituric acid-reactive substances

* Corresponding authors. fax: +358 8 553 1141.

E-mail addresses: vasily.antonenkov@oulu.fi (V.D. Antonenkov), kalervo.hiltunen@oulu.fi (J.K. Hiltunen).

<http://dx.doi.org/10.1016/j.ydbio.2014.03.022>

0012-1606/© 2014 Elsevier Inc. All rights reserved.

invasion into mammary stroma starts after initiation of puberty. After the onset of puberty the epithelial growth depends strictly on estradiol and progesterone (Neville et al., 2002). In addition, several other endocrine and paracrine factors are involved in the regulation of growth and maturation of mammary epithelium (Howlin et al., 2006; Ciarloni et al., 2007). Studies on developing postnatal mammary gland have revealed instructive and permissive interactions between mesenchymal and epithelial cells. Thus, the stromal tissue plays an important regulatory role in epithelial development and, in addition, provides vital metabolic assistance to the growing epithelial cells (Landskroner-Eiger et al., 2010).

Peroxisomes are oxidative organelles found in cells of all eukaryotes. The unique feature of these particles is their role in the metabolism of amphipathic molecules poorly soluble in water and in lipids such as fatty acids, some steroids and amino acids (Antonenkov et al., 2010). The main function of mammalian peroxisomes is the oxidation of long- and very-long-chain fatty acids (VLCFA), including branched-chain fatty acids (phytanic acid) and a side chain of bile acid precursors (di- and trihydroxycoprostanoyl-CoA). Accordingly, severe diseases (Zellweger syndrome, X-linked adrenoleukodystrophy, infantile Refsum's disease, rhizomeric chondrodysplasia punctata) are known to be caused by malfunctions of peroxisomes (Wanders and Waterham, 2006). One of the causative factors leading to deficiency of peroxisomal function might be restrictions in the transfer of metabolites across the peroxisomal membrane that would result in general (whole organism) or local (individual organs) metabolic disturbances (Antonenkov and Hiltunen, 2012). For instance, X-linked adrenoleukodystrophy is apparently caused by failure in the transmembrane transfer of VLCFA. However, diseases linked to the transfer of other peroxisomal metabolites have not yet been described.

Pxmp2, known also as PMP22, is an abundant 22 kDa membrane protein in mammalian peroxisomes. We have recently described the function of this protein as a transport channel with a pore diameter of 1.4 nm (Rokka et al., 2009). The channel conducts small solutes with a molecular mass up to 500 Da, but is unable to transfer 'bulky' compounds such as ATP and some cofactors (NAD/H, NADP/H, CoA and its acylated derivatives). Phenotypic analysis revealed a failure of Pxmp2-deficient female mice to nurse their pups due to severely retarded pubertal development of their mammary glands. Interestingly, our subsequent tissue transplantation experiments revealed that the mammary phenotype of Pxmp2^{-/-} mice was caused by abnormalities of the mammary stroma, and not the epithelium itself. We hypothesized that the deficiency in the function of fat pad peroxisomes in mice lacking the Pxmp2 channel causes deregulation of lipid homeostasis that in turn may lead to arrest of epithelial growth. This hypothesis was supported by lipidomics analysis of mammary fat pad. To our knowledge this is the first study to describe a peroxisomal protein that is indispensable for normal mammary gland development.

Materials and methods

Animal care and treatment

Mice were kept under germ-free conditions with a 12-h light/dark cycle and free access to food and water. All animal care and handling procedures were approved by the National Animal Experiment Board of Finland. The generation of Pxmp2-deficient mice has been described previously (Rokka et al., 2009). Briefly, Pxmp2 was disrupted by insertion of a LacZ-PGKneo-cassette into exon 2. The linearized targeting vector was electroporated into 129/SvJRW4 ES cells and recombinant ES cell clones were used for aggregation with C57BL/6J morulas. The Pxmp2^{+/-} germline offspring identified by RT-PCR analysis of tail-tip genomic DNA, were backcrossed with

C57BL/6J mice for 7 generations. The Pxmp2^{-/-} progeny were produced by mating Pxmp2^{-/-} male and Pxmp2^{+/-} female mice. For dated pregnancies, the female mice were mated and inspected daily for vaginal plugs. The day after copulation was counted as day 0.5 of pregnancy. Cross-fostering experiments were carried out just after the birth of pups and whole litters (up to 8 pups) were transferred.

For *in vivo* treatment, wild-type 4-months-old female mice were kept on a laboratory chow containing 0.5% (w/w) phytol (Sigma-Aldrich) for 12 weeks or 0.5% (w/w) clofibrate (ICN Biochemicals) for 14 days. To study the effect of antioxidants (Lopez-Erauskin et al., 2011), C57BL/6J and Pxmp2^{-/-} female mice were kept on AIN76A chow supplied with 1050 IU/kg α -tocopherol (Sigma) and 0.5% (w/w) α -lipoic acid (Sigma). The antioxidant-containing chow was prepared by SSniff GmbH (Germany). Additionally, mice received 1.0% (w/v) *N*-acetyl-L-cysteine, (Sigma-Aldrich) in drinking water, pH 3.5. The diet started at 3-weeks-of-age and ended at 10 weeks-of-age when mice were sacrificed. The mice in the control groups were kept on the same chow, but without added antioxidants.

Transplantation experiments

Three types of transplantations were performed using 3-weeks-old mice (Briskin et al., 1998). Each transplantation surgery was prepared using a separate recipient mouse. For whole mammary gland transplantation, the inguinal glands of donor mice were dissected and placed onto the abdominal wall under the ventral skin of recipient mice. For transplantation of mammary epithelium, the fat pads of inguinal glands in recipient mice were cleared. An incision was made in the cleared fat pad and a piece of mammary tissue of about 1.0 mm from the nipple region of a donor female was implanted. For fat pad transplantation the cleared fat pad from an inguinal mammary gland of a donor female with an inserted piece of the mammary tissue from another donor mouse were placed onto the abdominal muscle wall of a recipient mouse. After 9 weeks the transplanted tissues and endogenous mammary glands were analyzed using whole-mount preparations.

Mammary gland whole mount

Mammary glands were excised, spread on a glass slide, fixed for a minimum of 2 h in Carnoy's solution, stained overnight in carmine alum stain, and were permanently mounted with Permount (Electron Microscopy Sciences). The ductal lengths were determined by measuring the distance from the nipple area to the leading edge of the ductal tree. The number of branches was counted in the whole mammary gland.

Histology and electron microscopy (EM)

Mammary glands were fixed in 4% (w/v) paraformaldehyde, embedded in paraffin and the sections (5.0 μ m thick) were stained with hematoxylin-eosin (H&E). Frozen sections of inguinal mammary glands were used for Oil red O staining. For transmission EM, tissue samples were fixed in 2.5% (w/v) glutaraldehyde, postfixed in 1.0% (w/v) osmium tetroxide, dehydrated in acetone and embedded in Epon Embed 812 (Electron Microscopy Science). To reveal peroxidase activity of catalase, tissue slices were incubated in alkaline DAB medium [0.1% (w/v) 3'3'-diaminobenzidine tetrahydrochloride (DAB, Sigma), 5.0% sucrose, and 0.02% (v/v) H₂O₂ in 50 mM Tris-HCl buffer, pH 7.6], and postfixed in 1% (w/v) osmium tetroxide (Hand, 1973).

Immunohistochemistry

Paraffin sections (5.0 μ m) of mammary glands were incubated in Antigen Unmasking Solution (Vector Laboratories). Sections were

then treated with 50% (v/v) methanol containing 1.0% (v/v) H₂O₂ to eliminate any endogenous peroxidase. For detection of whey acidic protein (WAP) and β -casein, the sections were incubated overnight at 4 °C with goat anti-WAP antibody (sc-14832, Santa Cruz Biotech) or with goat anti- β -casein antibody (sc-17971, Santa Cruz Biotech), respectively. A Vectastain ABC Elite kit (Vector Laboratories) was used for detection of antibodies. For detection of cell proliferation mice were injected with BrdU (100 μ g/g body weight, Sigma-Aldrich) 2 h before sacrifice. Paraffin sections (5.0 μ m) of mammary glands were rehydrated and antigen retrieval was conducted using 3.0 mM citrate buffer, pH 6.0. After treatment with 3.0% (v/v) H₂O₂ to remove endogenous peroxidase activity, the sections were incubated with rat monoclonal anti-BrdU antibody (OBT 0030G, AbD Serotec) overnight at 4 °C. A similar procedure was applied for pro-apoptotic protein activated caspase-3 using rabbit anti-human caspase-3 antibody (#9661, Cell Signaling Technology). The proportion of BrdU-positive cells was determined as the number of brown stained mammary epithelial cells divided by the total number of mammary epithelial cells.

X-Gal staining

Tissue samples were incubated with a fixative solution [0.2% (v/v) glutaraldehyde, 2.0 mM MgCl₂ in 100 mM potassium phosphate buffer, pH 7.3] for 2 h, rinsed in washing buffer [0.01% (w/v) sodium deoxycholate, 0.02% (v/v) NP-40, 2.0 mM MgCl₂ in 100 mM potassium phosphate buffer, pH 7.3], and stained overnight with X-Gal buffer [1.0 mg/ml X-Gal (Sigma-Aldrich), 10 mM K₄Fe(CN)₆, 10 mM K₃Fe(CN)₆, 0.01% (w/v) sodium deoxycholate, 0.02% (v/v) NP-40, 2.0 mM MgCl₂ in 100 mM potassium phosphate buffer, pH 7.3]. After rinsing with washing buffer the samples were processed for H&E staining.

Hormone analysis

Blood was collected using retro-orbital bleeding. Serum progesterone was detected by an automated chemiluminescence system (Advia Centaur, Bayer Corporation) and estradiol was analyzed by a radioimmunoassay technique (Orion Diagnostic).

Serum and urine biochemical measurements

Mice were weighed and then anesthetized by intraperitoneal administration (10 μ g/g body weight) of a mixture of 0.7% (w/v) Ketalar (Pfizer) and 0.004% (w/v) Domitor (Orion Pharma). Blood was collected using a retroorbital bleeding technique with subsequent euthanasia by cervical dislocation and harvesting of the bile and tissues. For urine collection, mice were placed in metabolic cages (model 3700M021, Tecniplast), and samples collected within 24 h. Serum total protein, cholesterol, bilirubin, triacylglycerols, creatinine, and uric acid and urinary total protein, creatinine, and uric acid as well as serum and urinary sodium, potassium and chloride ions were measured on a Cobas Integra 700 automatic analyzer (Hoffman-LaRoche).

Detection of fatty acids, bile acid derivatives, complex lipids and polyamines

Serum fatty acids were extracted and detected as described (Savolainen et al., 2004). Samples from 5-weeks-old female mice were used for analysis of the total fatty acids and complex lipids in the mammary fat pad tissue. Mice of this age still contain only a rudimentary ductal system that allows removal of the fat pad samples without any admixture of mammary epithelium. In addition, the metabolic effects of the estrous cycle are expected to be minimal in mice at this age (Cohen et al., 2002). For analysis

of the total fatty acids the fat pad samples were homogenized in methanol/chloroform (6:1, v/v). The resulting homogenate was centrifuged, 1.4 ml aliquots of supernatant were mixed with 1.6 ml chloroform and 0.4 ml water, and 20 μ l of 2.5 mM nonadecanoic acid methylester (Sigma-Aldrich) was added as an internal standard. After mixing and centrifugation, 1.5 ml of the lower phase was evaporated to dryness under a stream of nitrogen at 60 °C. The residue was re-dissolved in 2.0 ml of 1.0 M HCl in methanol. After heating for 3 h at 75 °C, the resulting fatty acid methylesters were extracted twice with hexane and the combined extracts were evaporated. The residue was re-dissolved in 100 μ l hexane, applied on a silica TLC plates (Merck), and developed using hexane/ethanol (7:3, v/v). Areas of the TLC plates containing fatty acid methylesters were visualized with iodine, the esters were extracted using ethanol and the extracts were evaporated. The residues were re-dissolved in 20 μ l dichloroethane and 1.0 μ l of this solution was used for GLC analysis. Each sample was measured twice using a Hewlett Packard 5890 gas chromatograph; first, with a Phenomenex Zebron capillary glc column ZB-1701 (Phenomenex) and then with a FS-FFAP-CB-0.25 column (CS-Chromatographie Service). Bile acid derivatives from serum were determined as described (Savolainen et al., 2004).

Detection of complex lipids in the mammary fat pads was performed by ZORA Biosciences. Tissue samples were homogenized in ice-cold 70% (v/v) methanol containing 1.0% (w/v) butyl-hydroxy-toluene. Lipids were extracted according to a modified Folch method (Ekroos, 2008) performed using a Hamilton Micro-lab Star robot (Jung et al., 2011). Samples were spiked with non-endogenous synthetic internal standards of known amounts and after lipid extraction were reconstituted in chloroform/methanol (1:2, v/v). Synthetic external standards were post-extract spiked to the extracts before mass-spectrometric analysis. Diacylglycerols, glycerophospholipids, and sphingomyelins were analyzed by shotgun analysis on a hybrid triple quadrupole/linear ion trap mass spectrometer (QTRAP 5500, AB SCIEX) equipped with a robotic nanoflow ion source (NanoMate HD, Advion Biosciences). The analyses were performed in both positive and negative ion modes using a multiple precursor ion-scanning and neutral loss based method (Ekroos et al., 2003). The mass-spectrometry data were processed using LipidView™ to produce a list of lipid names and peak areas. A stringent cutoff was applied to separate background noise from actual lipid peaks. Lipids were normalized to their respective internal standard and to sample amount to retrieve their concentrations. A lipid was included in the analysis if it was detected at least in 4 samples in both groups.

Polyamines were quantified using an HPLC technique essentially as described (Pirinen et al., 2007). For sample preparation, mammary glands or pellets of red blood cells were homogenized in 25 mM Tris-HCl buffer, pH 7.4 containing 0.1 mM EDTA and 1.0 mM DTT. Proteins were precipitated with 5.0% (v/v) sulfosalicylic acid and the supernatant was analyzed. 10 μ m diaminoheptane (Sigma-Aldrich) was used as an internal standard.

Cell fractionation

Samples of fat pad tissue were collected from inguinal mammary glands and homogenates were prepared as described (Antononkov et al., 2004). Nuclear and cell debris were removed by centrifugation at 800g for 10 min. The total membrane fraction was isolated by centrifugation of the resulting supernatant at 100 000g for 1 h. The sediment was re-suspended in a small volume of isolation medium, loaded onto a linear 20–40% (v/v) Optiprep gradient (total volume ~11 ml) and centrifuged at 100 000g for 2 h. Fractions of 1.0 ml were collected.

Electrophysiological measurements

Single-channel analysis of P $xmp2$ was conducted essentially as described (Rokka et al., 2009). For measurements of reversal potential a two-fold (1.0 M KCl *trans*/0.5 M KCl *cis* compartment) salt gradient was established after insertion of a single channel into a stable lipid bilayer. Membrane proteins were solubilized in 0.5% (w/v) Genapol X-080 (Fluka).

Reverse transcription and quantitative RT-PCR analysis

Total RNA was isolated from mammary fat pad, liver or kidney of individual mice (four mice per group) using an RNeasy Lipid Tissue Mini Kit (Qiagen). The cDNA equivalent of 3.0 μ g RNA was produced using a RevertAid First Strand cDNA Synthesis Kit (Fermentas). Quantitative RT-PCR was performed with a 7500 Real Time PCR System (Applied Biosystems) according to the manufacturer's instructions. Expression levels of genes for peroxisomal proteins: urate oxidase (*Uox*, sequence accession number: NM_008993); xanthine oxidoreductase (*Xor*, XM_192827); 70 kDa peroxisomal membrane protein (*Pmp70*, NM_008991); catalase (*Cat*, NM_009804); carnitine acetyltransferase (*Crat*, NM_007760); straight- and branched-chain fatty acid oxidases (*Acox1*, NM_015729 and *Acox2*, NM_053115, respectively); multifunctional enzymes 1 and 2 (*MFE1*, AK004867 and *MFE2*, NM_008292, respectively), and polyamine oxidase (*Paox*, NM_153783) were detected. For relative quantification of gene expression, the results were normalized to the 18S rRNA or β actin levels.

SDS-PAGE and Western blotting

Tissue homogenates (20%, w/v) were prepared in 20 mM phosphate buffer, pH 7.4 and centrifuged at 800g for 10 min to eliminate cellular debris. Proteins were separated by SDS-PAGE under reducing conditions using 15% (w/v) acrylamide gels (Criterion Precast Gel, Bio-Rad) and electroblotted onto nitrocellulose filters (0.45 μ m Protran, Schlechter&Schuell). The filters were stained with specific antibodies against estrogen receptor α (ER α , H-184) than stripped of these antibodies and stained with anti- β -actin antibodies (sc-1616, Santa Cruz Biotechnology). MCF whole cell lysate was used in the same experiments as a positive control (Santa Cruz Biotechnology). Antibody prepared in rabbits against a synthetic peptide corresponding to the N-terminus of mouse P $xmp2$ (NH₂-APAASRLRVESELG) was also used. The locations of the primary antibodies were visualized using alkaline phosphatase-labeled anti-rabbit IgG (P $xmp2$ antibodies, Sigma-Aldrich) or the ECL chemiluminescence kit (other antibodies, Amersham).

Other methods

Thiobarbituric acid-reactive substances (TBA-RS) and the content of sulfhydryl groups were detected as described (Fernandes et al., 2010). The activity of marker enzymes and protein content were determined as described previously (Rokka et al., 2009).

Statistical analysis

All values are expressed as mean \pm standard deviation (SD). The data were analyzed by Student's *t* test (two-tailed). *P*-values less than 0.05 were considered significant. In case of complex lipid detection procedure the normality was not assumed because of low sample size and the analysis was performed using a non-parametric two group comparison—Wilcoxon matched pairs test.

Results

General phenotype of P $xmp2$ -deficient mice

To generate P $xmp2$ -deficient mice the LacZ-PGKneo-cassette was selectively inserted into exon 2 of P $xmp2$ using homologous recombination in mouse stem cells (see Rokka et al., 2009 for details). Breeding of heterozygous (P $xmp2$ ^{+/-}) mice gave wild-type, heterozygous, and homozygous (P $xmp2$ ^{-/-}) progeny at the expected Mendelian frequency. Overall, we did not detect any major alterations in the phenotype of P $xmp2$ ^{-/-} animals with the exception of retarded development of the mammary glands in female mice (see below). There were no identified abnormalities in gross appearance, gait or physical activity of P $xmp2$ -deficient mice. The body weights and the weight and appearance of organs (brain, heart, kidney, liver, and spleen) from P $xmp2$ ^{-/-} mice were similar to those of wild-type animals. Histological analysis (H&E staining) did not reveal any significant alterations in the major tissues examined. Liver function was normal, as indicated by GOT, GPT, and bilirubin serum levels. During EM examination of different tissues we noted flattening and fusion of podocyte foot processes in kidney of P $xmp2$ ^{-/-} mice, while liver and heart cells showed normal morphology (data not shown). A variety of biochemical parameters were tested in blood and urine (Supplementary Table S1). The only difference observed was an elevated level of uric acid in the blood of P $xmp2$ ^{-/-} mice. Peroxisomes contain polyamine oxidase (Wu et al., 2003), an enzyme involved in the maintenance of steady-state concentrations of polyamines – putrescine, spermidine, and spermine – which are regulators of cell growth and differentiation (Moinard et al., 2005). Measurement of polyamine levels in erythrocytes and mammary glands of 5 weeks-old females did not reveal substantial differences between groups of P $xmp2$ -deficient and wild-type mice with the exception of statistically significant changes in the content of spermine (Supplementary Fig. S1).

P $xmp2$ -deficient female mice produce pups but are unable to nurse them

P $xmp2$ -deficient mice showed normal fertility and produced full-term litters. The number, sex distribution, and weight of fetuses, as well as the average litter size, and the weight of newborn pups were indistinguishable between P $xmp2$ ^{-/-} and wild-type mice (data not shown). However, it was apparent that the P $xmp2$ ^{-/-} dams were able to nurse only very few pups. The P $xmp2$ ^{-/-} dams exhibited normal nursing behavior immediately after parturition, but all the pups regardless of their genotype failed to thrive and most of them died within 24 h post partum, despite repeated suckling attempts (Supplementary Fig. S2A and B). Cross-fostering experiments showed that when the pups of P $xmp2$ ^{-/-} females were foster-nursed by wild-type dams immediately after their birth, most of them survived. In contrast, none of the pups born to wild-type females were found alive 24 h after being transferred to P $xmp2$ -deficient foster dams (Supplementary Fig. S2C). These results indicate a possible failure in lactation of nursing P $xmp2$ ^{-/-} female mice. However, we did not find any abnormalities in the nursing of pups by heterozygous, P $xmp2$ ^{+/-} female mice (data not shown).

Mammary glands of P $xmp2$ -deficient mice are underdeveloped but produce milk

To identify the cause of the lactation defect, we first analyzed histological samples obtained at lactation day one. In P $xmp2$ ^{-/-} dams the mammary gland epithelium was poorly developed and consisted only of a ductal rudiment (Fig. 1A and B). This was confirmed by detection of the total protein content per g of

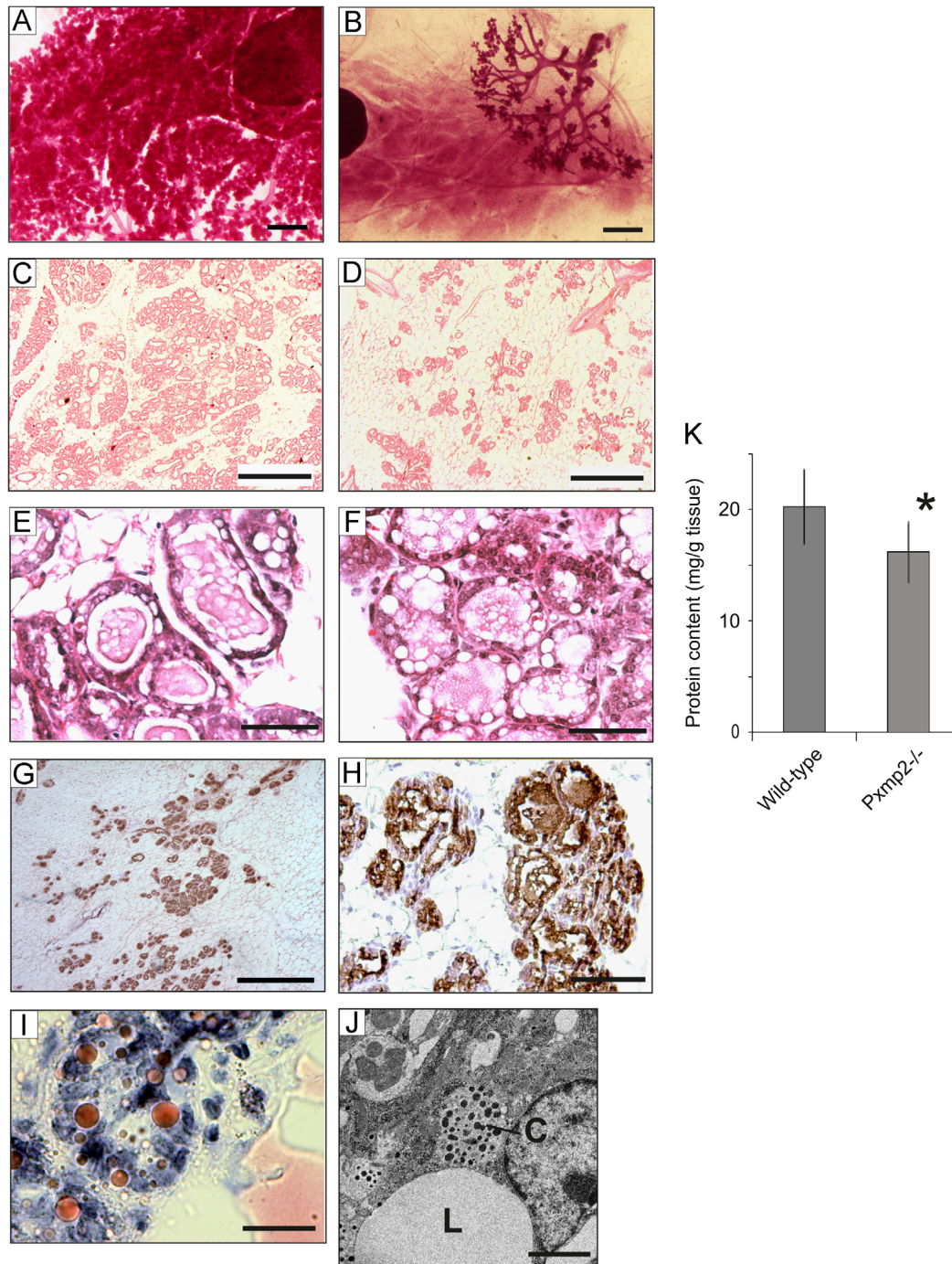


Fig. 1. Analysis of mammary gland development and function on lactation day 1. (A and B) Whole-mount preparation of inguinal glands from wild-type (A) and *Pxmp2*-deficient (B) mice, scale bar: 1 mm. (C–F) H&E stained sections of mammary glands from wild-type (C and E) and *Pxmp2*^{-/-} (D and F) mice at low (C and D) and high (E and F) resolution, scale bars: 500 μ m (C and D) and 50 μ m (E and F). (G and H) Immunohistological staining of *Pxmp2*^{-/-} mammary glands for milk proteins: β -casein (G) and WAP (H), scale bars: 500 μ m (G) and 100 μ m (H). (I) Oil Red O staining for milk fat, bar: 20 μ m. (J) EM of mammary gland epithelium from *Pxmp2*^{-/-} mice. L—lipid droplets; C—casein micelles, bar: 2000 nm. Each experimental group (A–J) contained 3–4 mice. (K) Protein content of the inguinal glands; * $P < 0.005$, $n = 12$ glands for each group. (For interpretation of the references to color in this figure legend, the reader is referred to the web version of this article.)

mammary gland tissue (Fig. 1K). In a normal lactating mammary gland the fat pad is completely filled with epithelium, highly enriched with milk proteins, and thus, the protein values obtained reflect the relative amount of epithelium in the gland. Although mammary gland growth in *Pxmp2*^{-/-} females was deficient, the rudimental ductal tree showed lobuloalveolar development, although the alveolar density was substantially decreased (Fig. 1A–D). Nevertheless, lipid droplets could be observed in the

mammary epithelial cells of *Pxmp2*-deficient mice (Fig. 1E and F). The ability of *Pxmp2*^{-/-} mammary epithelium to produce milk was confirmed by detection of two key protein components of the milk, β -casein and WAP (Fig. 1G and H) as well as milk fat (Fig. 1I) in the mammary gland sections. These data were further confirmed by EM examination of the epithelial cells (Fig. 1J). However, detailed analysis of milk content was not carried out because milking of *Pxmp2*^{-/-} females post partum was unsuccessful.

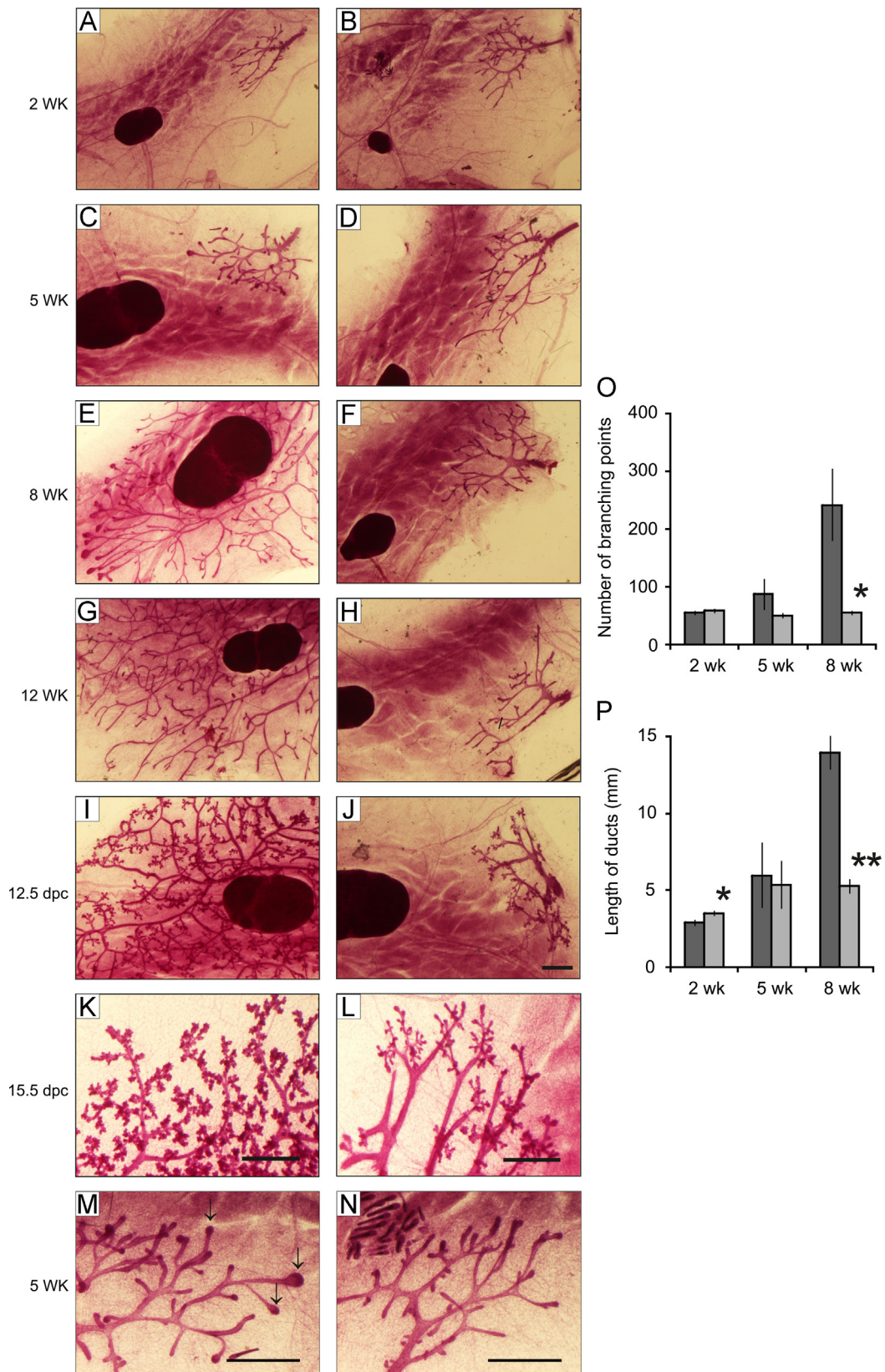


Fig. 2. Age-dependence of mammary gland development. Left panels: wild-type mice, right panels: *Pxmp2*-deficient mice. Age of mice (in weeks, WK) or date of pregnancy (dps) are shown on the left side of panels. (A–J) Whole mount micrographs of inguinal glands were prepared at the following developmental steps: 2 weeks (WK) after birth (A and B), 5 weeks (C and D), 8 weeks (E and F), 12 weeks (G and H), and 12.5 days (12.5 dpc) of pregnancy (I and J) at the same magnification, bar: 1.0 mm. (K and L) Whole mount preparations demonstrate reduced alveolar density and deficiency in the number of branching points in the inguinal glands of *Pxmp2*^{-/-} mice (L) relative to wild-type females (K) at 15.5 days of pregnancy, bar: 1.0 mm. (M and N) Pubertal mouse (5 week old) inguinal glands showing individual mammary ducts that terminate in undeveloped terminal end buds in *Pxmp2*^{-/-} mice (N), arrows indicate the well-developed terminal end buds in mammary glands of wild-type mice at the same age (M), bar: 1.0 mm. (O) Number of branching points and (P) an average length of ducts in inguinal mammary glands of females at different ages. At least three mice of each genotype were analyzed; * $P < 0.05$, ** $P < 0.002$.

Age-dependence of mammary gland development

To assess whether or not a defect in the growth of mammary epithelium was specifically linked to a certain time-point of mouse maturation we analyzed mammary glands of *Pxmp2*^{-/-} mice at critical developmental stages using a whole-mount technique (Fig. 2). Importantly, no differences in the morphology of inguinal mammary glands could be observed at the age of 2 weeks (Fig. 2A and B), demonstrating that embryonic and pre-pubertal development of mammary glands proceeded similarly in wild-type and *Pxmp2*^{-/-} mice. After the onset of puberty, as verified by detection of a vaginal opening (at the age of 23 ± 1 and 23 ± 2 days in wild-type [*n*=31] and *Pxmp2*^{-/-} [*n*=23] mice, respectively), appearance of terminal end buds (TEBs) was analyzed in the mammary epithelium. In wild-type mice TEBs were detected at 5 weeks of age (Fig. 2C, E and M) and, consequently, ductal elongation proceeded until the epithelia filled the entire stroma by the age of 12 weeks (Fig. 2C, E, G, O and P). In contrast, no TEBs were formed in the mammary glands of *Pxmp2*^{-/-} mice and the mammary epithelial tree remained as a ductal rudiment and failed to fill the mammary fat pad (Fig. 2D, F, H, N, O and P). During pregnancy, despite significant growth retardation, the ductal system of *Pxmp2*^{-/-} mammary glands showed side branching and alveologensis (Fig. 2I–L). To assess the possibility of estradiol and progesterone causing the *Pxmp2*-dependent phenotype we measured the levels of these hormones in serum of mice at different ages (Supplementary Table S2). No difference were observed between the age-matched groups of *Pxmp2*^{-/-} and wild-type animals, indicating no effects on estradiol and progesterone levels in *Pxmp2*^{-/-} mice, caused e.g. by hypothalamic-pituitary and/or ovarian aberrations. Taken together, our results

indicate that *Pxmp2* has no systemic effects on sexual maturation, but it is indispensable for mammary ductal growth during puberty. However, the terminal differentiation of the existing epithelial cells in the rudimentary glands is not affected. Contrary to *Pxmp2*^{-/-} female mice, we did not find a marked retardation in the epithelial growth of the heterozygous, *Pxmp2*^{+/-}, mice (Supplementary Fig. S3).

Pxmp2 deficiency affects proliferation of mammary gland epithelium

The inability of the ductal tree to grow in *Pxmp2*-deficient mammary glands may be a result of an insufficient proliferation of epithelial cells and/or increased apoptosis. Therefore, we analyzed the proliferative and apoptotic indices of the inguinal mammary glands of 5-weeks-old mice by BrdU incorporation and immunohistochemistry for activated caspase 3, respectively. On average, 16% of the cells in the epithelium of wild-type mammary glands were in S phase, whereas in *Pxmp2*^{-/-} glands, only 1.0% of the cells incorporated BrdU (Fig. 3 and Supplementary Fig. S4). In contrast, caspase 3 immunostaining showed no difference between genotypes (data not shown) indicating that the growth defect does not depend on increased apoptosis but, instead, results from defective proliferation.

The fat pad is responsible for deficient proliferation of mammary gland epithelium

By using tissue transplantation experiments we aimed to reveal whether the factors affecting development of *Pxmp2*^{-/-} mammary glands were either of: (i) systemic (other than estradiol and progesterone), (ii) epithelial or (iii) stromal origin. Transfer of

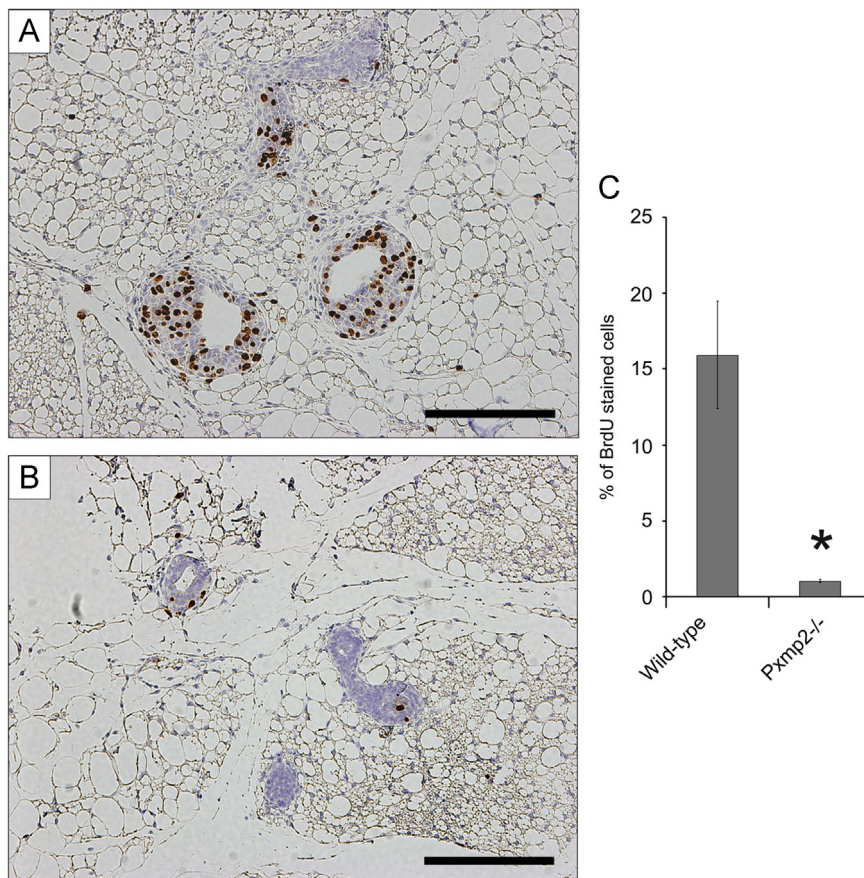


Fig. 3. Epithelial proliferation in mammary glands. Histological sections of mammary glands from wild-type (A) and *Pxmp2*^{-/-} (B) mice stained with an anti-BrdU antibody, bar: 200 μm. (C) The relative numbers of BrdU-positive mammary epithelial cells, at least 5000 cells were counted in each group; **p* < 0.05, *n* = 4 mice per group.

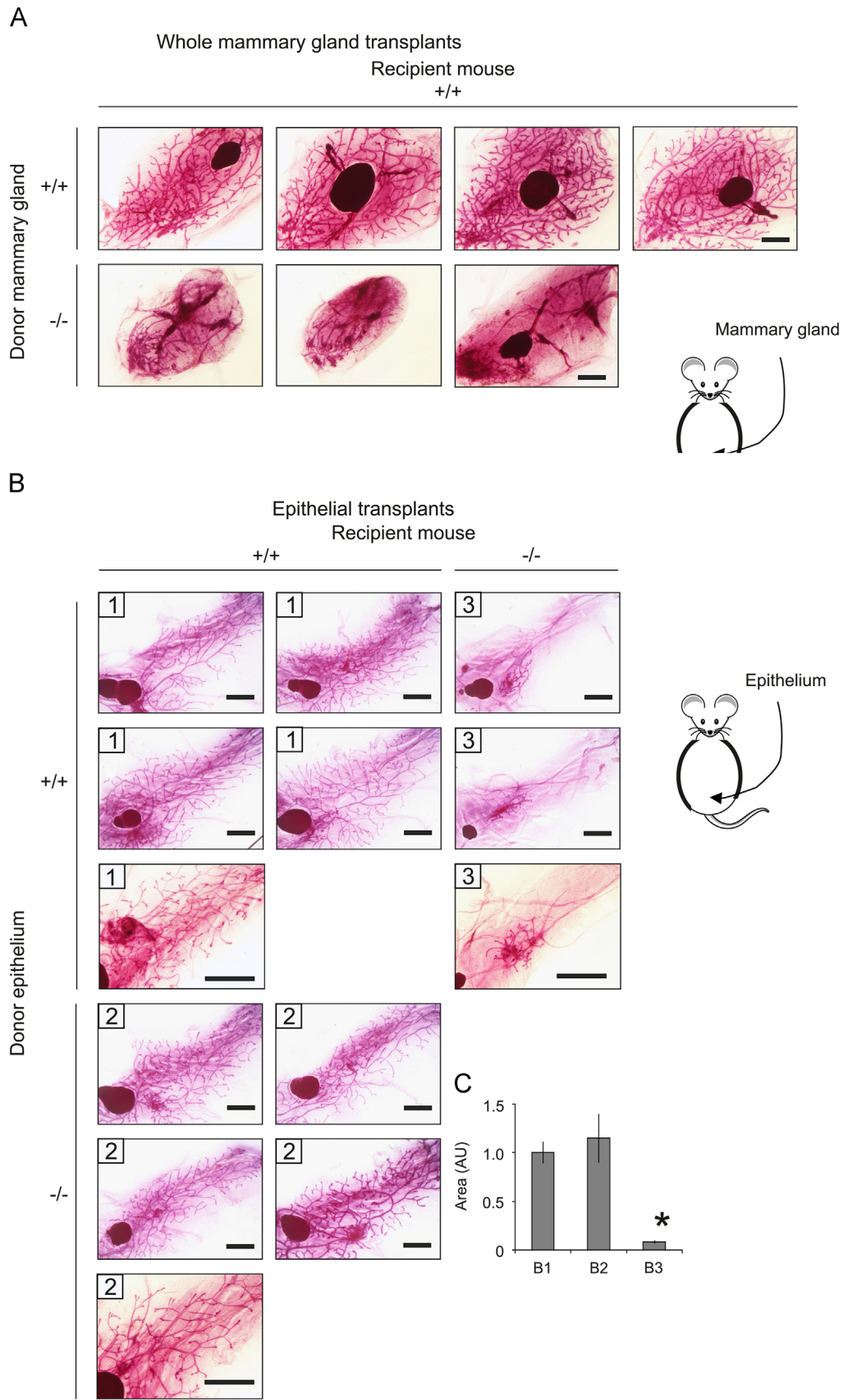


Fig. 4. Mammary gland reconstitution experiments. Results (whole mount) of the transplantation of whole mammary glands (A), epithelium (B) or epithelium and fat pad (D) to recipient mice are presented; bars: 1.0 mm. All grafts that have been produced in reconstitution experiments are shown. Diagrams of transplantation experiments are also shown. Genotype of mice and transplants is marked as: +/+, wild-type; -/-, *Pxmp2*-deficient. (B) Three groups of mice with different genotype were analyzed: 1—wild-type donor epithelium/wild-type recipient mouse; 2—*Pxmp2*^{-/-} donor epithelium/wild-type recipient mouse; 3—wild-type donor epithelium/*Pxmp2*-deficient recipient mouse. (C) Total area of epithelial outgrowth (in arbitrary units, AU) after transplantation of epithelium (B, panels 1–3). **P* < 0.001 if compared with control transplantations (B1). (D) Groups of mice according to genotype in the reconstitution experiments: 1—wild-type donor epithelium/wild-type donor fat pad/wild-type recipient mouse; 2—*Pxmp2*^{-/-} donor epithelium/wild-type donor fat pad/*Pxmp2*^{-/-} recipient mouse; 3—wild-type donor epithelium/*Pxmp2*^{-/-} fat pad/wild-type recipient mouse. (E) Total number of branching points was analyzed in grafts shown on (D). **P* < 0.01 if compared with control transplantations (D1).

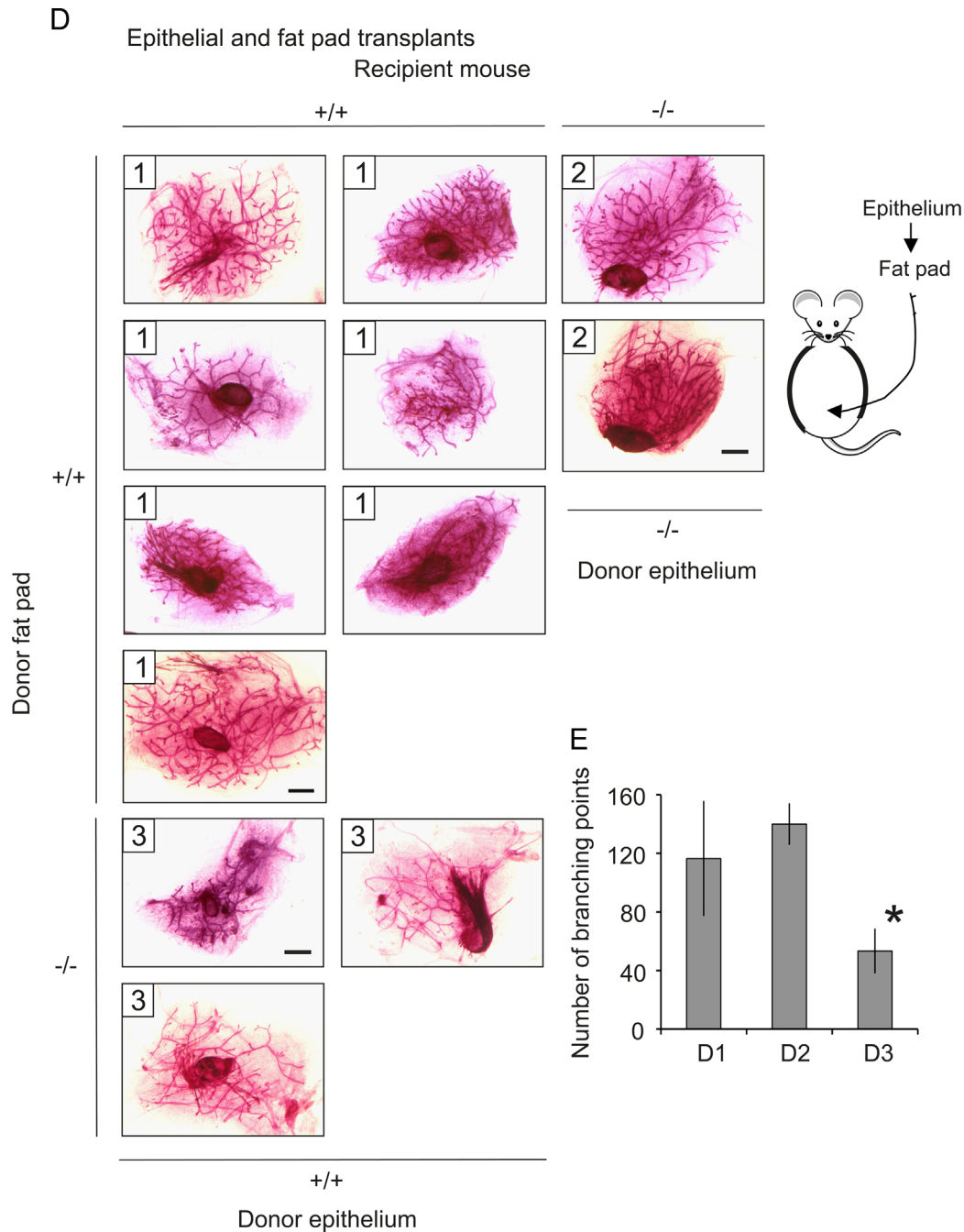


Fig. 4. (continued)

whole mammary glands from wild-type and *Pxmp2*-deficient donor mice into wild-type recipient mice showed development of wild-type but failure with *Pxmp2*^{-/-} donor tissue (Fig. 4A—the figure shows the results of all executed transplantation experiments). Minor necrotic transformations were detected as a result of transplantation experiments, however these changes did not prevent growth of the donor mammary glands as can be seen using the wild-type transplants (Fig. 4A). Whole mammary gland transplantation experiments ruled out a systemic factor(s), caused by *Pxmp2* deficiency as the source of the observed mammary phenotype, but instead pointed to a local, tissue level defect in the mammary gland. Next, we determined whether the growth defect was of paracrine nature originating from the mammary stroma, or whether it was caused by autocrine stimuli in the epithelial compartment itself. A small piece of mammary epithelium from

a *Pxmp2*^{-/-} or wild-type female was transplanted into the fat pad of 3-week-old virgin mice, cleared from its own epithelium (Fig. 4B, panels 1–3). In this type of experiments the necrotic changes were only barely detectable. The transplantations allow the donor epithelium to penetrate the host fat pad and become associated with the recipient stroma. Results showed that the *Pxmp2*^{-/-} epithelium was able to fully elongate when it was inside a wild-type mammary fat pad (Fig. 4B, panels 2). In contrast, transplantation of wild-type epithelium into a *Pxmp2*^{-/-} fat pad resulted only in a rudimentary ductal tree, which failed to fill the surrounding normal fat pad (Fig. 4B, panels 3). These data were confirmed by quantitative estimation of the total area of epithelial outgrowth after transplantation (Fig. 4C). Results of the transplantation experiments using as donor tissues the whole mammary gland (Fig. 4A) and the mammary epithelium (Fig. 4B and C) are

sufficient to conclude that the deficient development of the *Pxmp2*^{-/-} epithelium is not caused by a defect in the epithelial cells *per se* but, instead, is associated with abnormalities in the mammary stroma. Finally, to confirm further a direct involvement of the *Pxmp2*^{-/-} fat pad in preventing normal growth of the mammary epithelium, we transplanted the cleared fat pad to a donor female mouse together with an inserted piece of epithelium from another donor mouse into a recipient mouse (Fig. 4D and E).

In five out of seven control transplantations (wild-type transplants and recipients; Fig. 4D, panels 1) an intensive epithelial outgrowth was detected. However, the growth was limited by the area of fat pad transplanted. The growth was also registered when *Pxmp2*^{-/-} epithelium was inserted into wild-type donor fat pad and transplanted into the *Pxmp2*-deficient mice (Fig. 4, panels 2). Epithelial growth was significantly reduced only if the epithelium was transplanted into a cleared *Pxmp2*^{-/-} fat pad in a wild-type

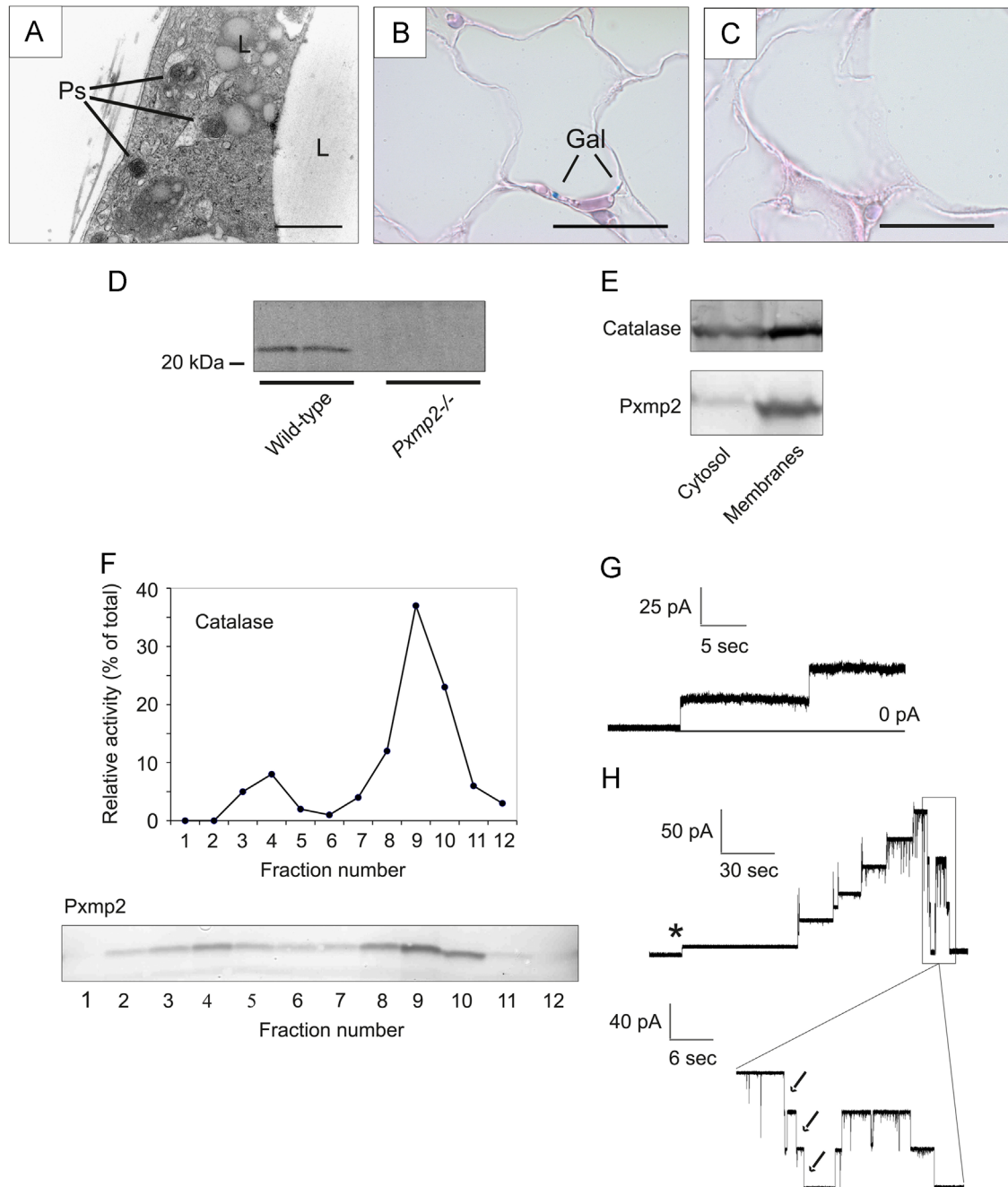


Fig. 5. Detection of peroxisomes and *Pxmp2* in fat pad of mammary glands. (A) Electron micrograph of adipocyte stained with DAB to reveal localization of catalase in peroxisomes. Ps—peroxisomes, L—lipid droplet; bar: 1.0 μ m. (B) β -Gal staining of *Pxmp2*^{-/-} fat pad. Dotted staining marked as Gal indicates presence of *Pxmp2* protein in the fat pad adipocytes; bar: 20 μ m. (C) Control β -Gal staining of wild-type adipocytes. (D) Fat pad homogenates from 2 mice of each genotype were subjected to SDS/PAGE followed by Western blotting with antibodies against *Pxmp2*. (E) Detection of catalase and *Pxmp2* proteins in cytosol and total membrane fraction of fat pad homogenate. (F) Linear Optiprep gradient of total membranes showing co-localization of catalase and *Pxmp2*. Upper panel: relative activity of catalase, the enzyme recovery was 102%; lower panel: proteins from equal volumes of each fraction were separated by SDS/PAGE and analyzed by immunoblotting using antibodies against *Pxmp2*. (G and H) Electrophysiological analysis of the '*Pxmp2*-like' channel detected in fractions enriched with fat pad peroxisomes (fractions 4, 9, and 10, see panel F). In all experiments 1.0 M KCl was used as an electrolyte. (G) Current trace of two channels registered at +20 mV. (H) Voltage-dependent gating of the channel. Insertion of a single channel (marked by asterisk) was registered at +10 mV and the voltage was then increased manually up to +110 mV with 10 mV intervals. The lower trace shows a timescale-expanded current record from the upper trace. Note spontaneous three-step closing of the channel (marked by arrows).

female recipient (Fig. 4D, panels 3 and Fig. 4E). Taken together, these experiments confirmed that the *Pxmp2*^{-/-} fat pad is solely responsible for defective development of the mammary epithelium.

Retarded mammary epithelial outgrowth due to *Pxmp2* deficiency is reminiscent of the phenotype of ER α knock-out mice (Malpell et al., 2006). However, only the epithelial receptor is required for proliferation and morphogenesis in the mammary gland which is in contrast with an involvement of the stromal *Pxmp2* protein in the same processes. We did not find any substantial difference in the ER α gene expression in fat pad (data not shown) or in the level of this protein in whole mammary gland or fat pad (Supplementary Fig. S4E and F) of wild-type and *Pxmp2*^{-/-} mice.

Detection of peroxisomes and *Pxmp2* in mammary fat pad

The mammary stroma of mice consists mainly of adipocytes (Landskroner-Eiger et al., 2010). Information about the presence of peroxisomes in these cells is lacking. Therefore, we examined samples using EM to determine whether peroxisomes could be identified in the adipocytes of mammary fat pad (Fig. 5A and Supplementary Fig. S5A). We observed small (diameter 0.2–0.3 μ m), DAB-positive round or oval particles surrounded by a single membrane, which are characteristic of peroxisomes. Next, we investigated the presence and localization of *Pxmp2* in fat pad cells. Several tissues from *Pxmp2*-deficient mice were stained for β -gal activity as the *LacZ* reporter gene coding for β -gal is a part of *LacZ*-PGKneo-cassette inserted into exon 2 of the *Pxmp2* to disrupt this gene. Specific staining for β -gal was detected in heart, kidney (Supplementary Fig. S5B), liver (data not shown), and in the mammary fat pad adipocytes (Fig. 5B) of *Pxmp2*^{-/-} mice but was not observed in samples from wild-type animals (Fig. 5C). This indicates that the *Pxmp2* gene is expressed in the tissues analyzed. These data corroborate with the observation that the *Pxmp2* gene is expressed in a wide range of different tissues analyzed with the highest level of expression in organs deeply involved in lipid metabolism, such as liver, heart, white and brown adipose tissues (V. Tillander and S.E.H. Alexson, personal communication). The presence of the *Pxmp2* protein in mammary fat pad homogenates from wild-type mice was confirmed by Western blotting (Fig. 5C). Analysis of the subcellular localization of *Pxmp2* revealed that, as expected, the protein is bound to membranes (Fig. 5D) and shares a pattern of distribution in an Optiprep gradient with the marker peroxisomal enzyme catalase (Fig. 5E and Supplementary Fig. S5C). These data indicate that *Pxmp2* is a peroxisomal membrane protein in fat pad tissue. To detect the activity of stromal *Pxmp2* as a functional membrane channel, proteins from gradient fractions enriched with peroxisomes were solubilized with detergent and subjected to electrophysiological analysis using the planar lipid bilayer technique. We took advantage of the single channel analysis to study the electrophysiological properties of only one channel molecule that allows the discrimination of different channel types in membrane preparations. Using this approach we identified channel-forming activity (Fig. 5F and G) with conductance (1.34 ± 0.04 nS slope conductance, 1.0 M KCl, $n=5$), cation selectivity ($E_{rev}=6.7$ mV, $P_{K/Cl} \approx 2.3$) and voltage dependence (three-step closure at voltages over ± 100 mV) very similar to those registered for the high-conductance form of a purified native *Pxmp2* (Rokka et al., 2009) indicating that fat pad *Pxmp2* is active as a membrane channel.

Effect of *Pxmp2* deficiency on lipid homeostasis

We hypothesized that deletion of the *Pxmp2* channel affects metabolic processes in peroxisomes by preventing free movement of small solutes across the peroxisomal membrane. This could lead

to disturbances in synthesis and degradation of metabolites in peroxisomes from different tissues including mammary fat pad and eventually results in negative nutritional or regulatory effects on the developing mammary epithelium. Because mammalian peroxisomes are heavily involved in lipid metabolism (Wanders and Waterham, 2006; Antonenkov et al., 2010), we focused on the comparative analysis of the content of different lipids in body fluids and in mammary fat pad of wild-type and *Pxmp2*-deficient mice. We first analyzed the concentration of free fatty acids in serum (Supplementary Table S3) and the content of bile acids in bile fluid (Supplementary Table S4). The data did not show any significant differences between the groups indicating that deletion of *Pxmp2* may not result in systemic changes in lipid metabolism in the whole organism under normal conditions. To investigate the phenotype of *Pxmp2*-deficient mice under dietary stress, animals were fed diets containing phytol, a natural methyl-branched acyl alcohol metabolized via α -oxidation only in peroxisomes (Wanders and Waterham, 2006) or clofibrate, a known proliferator of rodent liver and kidney peroxisomes (Reddy and Hashimoto, 2001). No weight gain or loss and no significant alterations in the morphological appearance of different tissues were detected in *Pxmp2*^{-/-} mice compared with wild-type animals consuming the same diet. Similarly, no difference was observed when fatty acids, including phytol metabolites: phytanic and pristanic acids were analyzed in serum (Supplementary Table S5). Consumption of clofibrate led to similar elevation in size and number of peroxisomes in liver and kidney of *Pxmp2*^{-/-} and wild-type mice (data not shown).

In contrast, *Pxmp2* deficiency led to local disturbances in the content of total fatty acids and the composition of complex lipids in the mammary fat pad. In particular, a two-fold decrease in the concentration of medium-chain myristic acid (C14:0) was registered (Fig. 6A and Supplementary Table S6). The fatty acid composition of complex lipids was affected as well (Fig. 6B and Supplementary Table S7). The hallmark observation was that the levels of a variety of diacylglycerols, phosphocholines, and phosphoethanolamines were decreased in the fat pad of *Pxmp2*^{-/-} mice versus wild-type animals (Fig. 6B). Interestingly, the rate of the decrease was almost linearly dependent on the number of double bonds in the fatty acids of diacylglycerols (Fig. 6C). This indicates that the registered changes in lipid concentrations are highly selective and does not result from a decrease in the total lipid content of fat pad cells. The latter was confirmed by analysis of the content of phospholipids depending on their fatty acid composition. As in the case of diacylglycerols, the fat pad phospholipids of *Pxmp2*-deficient mice contained much less polyunsaturated fatty acids compared to those of wild-type animals (Fig. 6D).

The data indicating disturbances in fat pad lipid homeostasis of *Pxmp2*^{-/-} mice were strengthened by gene expression analysis of some peroxisomal proteins (Fig. 6E and Supplementary Fig. S6). The reason for this analysis was a well-known ability of mammalian cells to regenerate function of metabolically compromised peroxisomes by activation of the synthesis of key peroxisomal enzymes (Reddy and Hashimoto, 2001). *Pxmp2* deficiency evidently affected the mRNA level of several peroxisomal proteins in the fat pad (Fig. 6E). Thus, the real time PCR analysis revealed an elevated content of mRNA for multifunctional enzyme 1, catalase, and acyl-CoA oxidase 1 in the *Pxmp2*-deficient versus wild-type mice. An elevated expression of peroxisomal proteins due to *Pxmp2* deficiency is a tissue-specific event since no differences were registered in liver and kidney of *Pxmp2*^{-/-} mice relative to wild-type animals (Supplementary Fig. S6).

Defective metabolism in microperoxisomes, especially in lipid-rich tissues like myelin, due to malfunctioning of the peroxisomal membrane transporter ABCD1 that causes the neurodegenerative inherited disease X-adrenoleukodystrophy is accompanied

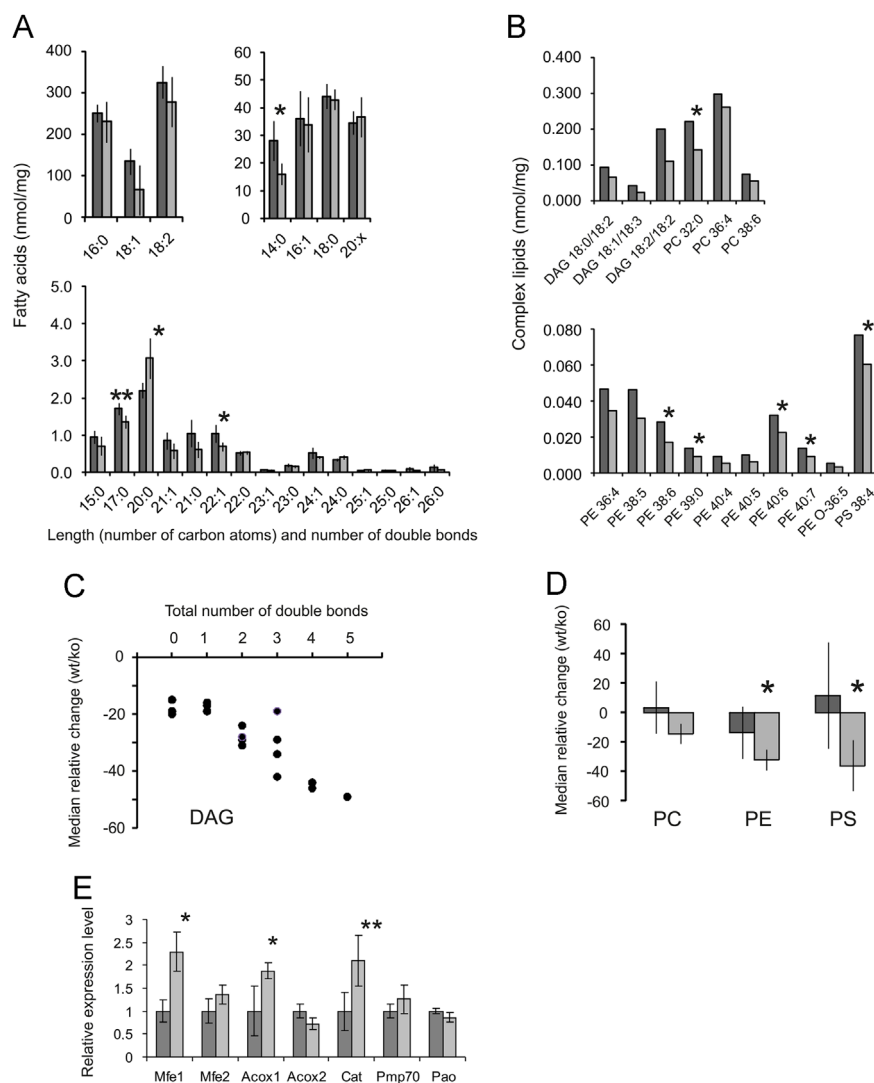


Fig. 6. Effect of *Pxdmp2* deficiency on the lipid content and the expression levels of selected peroxisomal genes in the mammary fat pad. Mammary fat pad of 5-week-old mice was used for analysis of lipids. (A) Total fatty acids content in mammary fat pad of wild-type (dark grey bars) and *Pxdmp2*^{-/-} (light grey bars) mice; $n=5$ in each group; $*P < 0.05$, $**P < 0.01$. Myristic acid is marked as 14:0. (B) Analysis of complex lipids in mammary fat pad of wild-type (dark grey bars) and *Pxdmp2*^{-/-} (light grey bars) mice; $n=4-6$. Only data showing a statistically significant difference between the analyzed groups are presented; $P < 0.05$ (not marked) or $P < 0.01$ (marked by an asterisk). The whole set of results is in [Supplementary Table S7](#). Wilcoxon matched pairs test was used for statistical analysis of the data. DAG, diacylglycerol; PC, phosphatidylcholine; PE, phosphatidylethanolamine; PE-O, alkyl-phosphatidylethanolamine; PS, phosphatidylserine. (C) Dependence between the decrease of DAG's concentration and the number of double bonds in fatty acid residues of corresponding DAG's in the *Pxdmp2*^{-/-} mammary fat pad relative to control (wild-type) samples. Note near linear correlation of these parameters. DAG's containing fatty acids of different length but with equal number of double bonds per molecule were combined in the corresponding groups. (D) Change in the phospholipid content in the fat pad of *Pxdmp2*^{-/-} relative to wild-type mice depending on the total amount of double bonds in fatty acids. All detected phospholipids in each class (see [Supplementary Table S7](#)) were separated into two groups: containing up to 3 double bonds (dark grey bars) and 4 or more double bonds (light grey bars). Length of fatty acids was not considered. The average deviation was calculated for each group; $*P < 0.05$, $n=5-8$. (E) Expression levels of genes in mammary fat pad of 5-week-old *Pxdmp2*^{-/-} mice (light grey bars) compared to those for wild-type control (dark grey bars) were analyzed by quantitative real-time PCR. Data are means \pm SD of 4–6 mice per group; $*P < 0.02$, $**P < 0.05$. Mfe1, multifunctional enzyme 1; Mfe2, multifunctional enzyme 2; Acox1, acyl-CoA oxidase; Acox2, pristanoyl-CoA oxidase; Cat, catalase; Pmp70, peroxisomal 70 kDa membrane protein; Pao, polyamine oxidase.

by oxidative damage from lipid peroxidation (Singh and Pujol, 2010). Similarly, deletion of a single allele of the *Pex11 β* gene coding for peroxisomal membrane protein Pex11 was sufficient to trigger oxidative stress and neuronal death in mouse brain (Ahlemeyer et al., 2012). Furthermore, a diet enriched with antioxidants reversed signs of neurodegeneration caused by ABCD1 deficiency (Lopez-Erauskin et al., 2011) indicating that oxidative stress may be a major disease-driving factor in the pathogenesis of X-adrenoleukodystrophy. Our results showing a decrease in the amount of polyunsaturated fatty acids in complex lipids, especially in phosphatidylserine (Tyurina et al., 2008) may indicate activation of lipid peroxidation in the fat pad of *Pxdmp2*^{-/-} mice. This information led to analysis of the content of oxidative

stress markers – TBA-RS and sulfhydryl groups – in the homogenates of mammary fat pad. We also tested whether a diet enriched with antioxidants would stimulate epithelial growth in mammary glands of transgenic mice. Detection of the oxidative stress indicators did not reveal a drastic difference between control and experimental groups of animals although the content of sulfhydryl groups was moderately decreased in the mammary fat pad of *Pxdmp2*^{-/-} mice ([Supplementary Fig. S7A](#)). In experiments with the antioxidant diet we did not observe any improvements in the development of mammary epithelium in transgenic mice ([Supplementary Fig. S7B–D](#)). Therefore, even when lipid peroxidation is activated in the *Pxdmp2*^{-/-} fat pad, this process seems to have little effect on epithelial development.

Discussion

Mammary gland development is a target of intensive research due to the importance of this organ in reproductive biology and the tremendous burden of mammary gland neoplasms among life threatening human diseases (Lanigan et al., 2007; McCready et al., 2010). Growth of mammary epithelium is connected to sexual development and includes embryonic, prepubertal and pubertal stages, as well as terminal differentiation during pregnancy, and lactation. More than fifty different genetically modified mouse lines have been created that display aberrant mammary gland development. Most of the identified factors regulating mammary growth are linked to endocrine status, stromal-epithelial cross talk and local signaling. The present work demonstrates that a deficiency in peroxisomal function, through generation of *Pxmp2* null mutant mice, results in failed mammary epithelial growth during puberty thus adding a novel category – peroxisomal metabolism – to the list of biological processes essential for normal development of mammary gland.

The transport network of the peroxisomal membrane represents a unique biological entity consisting of both, pore-forming channels carrying ‘small’ solutes and transporters specific for certain ‘bulky’ solutes (Antonenkov and Hiltunen, 2012). *Pxmp2* encodes a peroxisomal membrane protein that forms a water-filled pore with an estimated diameter of 1.4 nm (Rokka et al., 2009) connecting the cytoplasm and the peroxisomal matrix. This channel is non-selective, i. e. it allows solutes with molecular masses up to 500 Da to diffuse across the peroxisomal membrane. Indeed, our *in vitro* experiments on peroxisomes isolated from the liver of *Pxmp2*-deficient mice revealed compromised transfer of solutes across the peroxisomal membrane (Rokka et al., 2009). Deficiency of the *Pxmp2* channel may disrupt intracellular solute traffic *in vivo* and, as a result, cause malfunctioning of peroxisomal metabolic machinery.

As shown in this study, *Pxmp2*^{-/-} mice were unable to nurse their pups due to retarded ductal outgrowth during puberty. Immunohistochemical analysis revealed that *Pxmp2* deletion specifically suppresses the proliferation of epithelial cells. However, while the mammary glands were severely undeveloped, the existing rudimentary epithelium was still able to respond to pregnancy hormones and to undergo terminal differentiation. Comprehensive tissue transplantation experiments showed that mammary fat pad was the tissue responsible for impaired development of the epithelium. We detected peroxisomes in stromal adipocytes and showed that the fat pad of wild-type mice contains *Pxmp2*, which was associated with peroxisomal membranes and was functionally active as a channel-forming protein. These data led us to suggest an involvement of fat pad *Pxmp2* in the regulation of mammary epithelial development.

Pxmp2 is a prominent component of mammalian peroxisomal membranes in liver and kidney, and its malfunctioning or deletion would predict severe consequences for peroxisomal function and ultimately for the whole organism. However, except suppressed mammary gland growth, only minor phenotypic changes of *Pxmp2* knock-out mice were detected. The mild phenotype implies that the peroxisomal membrane contains additional channel-forming proteins with overlapping functions. Indeed, our previous studies have shown the presence of several different channel-forming activities in mammalian and yeast peroxisomes (Antonenkov and Hiltunen, 2012). As have been shown recently in our experiments, these channel-forming activities are carried out by members of the *Pex11* family of peroxisomal membrane proteins (Manuscript in preparation). This is likely to lead to functional redundancy of peroxisomal channels in most tissues preventing evident malfunctioning of peroxisomes in *Pxmp2*^{-/-} mice. The functional redundancy of several mammalian peroxisomal proteins has been well documented (Baes and Van Veldhoven, 2012). A poor phenotype was observed when the knock-out mouse models for multifunctional enzyme type 1 (Qi et al., 1999), α -

methylacyl-CoA racemase (Savolainen et al., 2004), and 3-oxoacyl-CoA thiolase B (Chevallard et al., 2004) were analyzed.

A deficiency of the *Pxmp2* channel has an effect on the development of mammary epithelium through dysfunction of mammary stroma, as shown by our transplantation experiments. This observation adds to the list of instances where the stroma influences epithelial outgrowth and differentiation. Different stromal cells including fibroblasts (Yang et al., 2006; Lanigan et al., 2007), adipocytes (Landskroner-Eiger et al., 2010), macrophages and eosinophils (Gouon-Evans et al., 2000) are required for proper postnatal development of the mammary epithelium. Members of the transforming growth factor beta (TGF β) family – inhibins and activins – were the first signaling molecules shown to regulate mammary epithelial outgrowth through stromal-epithelial interaction (Robinson and Hennighausen, 1997). An important regulatory axis is paracrine signaling triggered by estrogen and conveyed by action of the epithelial ER α , amphiregulin and the stromal epidermal growth factor receptor (Wiesen et al., 1999; Mallepell et al., 2006; Sternlicht and Sunnarborg, 2008). Interestingly, a growing number of observations revealed tissue- and cell-specific manifestations of the malfunctioning of peroxisomes and dependence of the adjacent tissues on peroxisomal functions (Baes and van Veldhoven, 2012). Thus, our findings on mammary glands coincide with the reports on the role of glial peroxisomes in maintaining the structural and functional integrity of neurons in the central nervous system. Genetic inactivation of peroxisomes in oligodendrocytes, which are the primary components of glia (Kassmann et al., 2007), but not in neurons or astrocytes (Bottelbergs et al., 2010) caused axonal degeneration and demyelination. It is important to note the similar role of these tissues: the mammary fat pad provides vital trophic and regulatory assistance to growing epithelium (Hovey and Aimo, 2010; McNally and Martin, 2011), and glial cells serve the same functions for the neuronal network (Kassmann et al., 2007). These observations indicate that fat pad and glial peroxisomes apparently have much in common in maintaining integrity of the mammary epithelium and the neuronal axons, respectively.

Since peroxisomes are crucially involved in lipid metabolism, one can predict that abnormalities in lipid homeostasis leading to trophic and/or regulatory malfunctioning of mammary fat pad are associated with an abnormal epithelial growth. Indeed, systemic diet-induced perturbations in lipid composition (Flint et al., 2005; Olson et al., 2010; Berryhill et al., 2012) as well as local deficiency of mammary adipocytes (Hovey and Aimo, 2010; Landskroner-Eiger et al., 2010) or separate lipid-metabolizing enzymes such as acyl-CoA:diacylglycerol transferase 1 (Cases et al., 2004) result in impaired mammary gland development. In addition to trophic assistance, some lipids play an important role in regulatory networks as ligands for nuclear and other receptors. One example is an involvement of peroxisome proliferator-activated receptors α and β (PPAR's) which use lipids as ligands (Schupp and Lazar, 2010), in the regulation of mammary gland development. Although PPAR α disruption is not associated with abnormal mammary growth (Lee et al., 1995), activation of this receptor during puberty (manuscript in preparation) and pregnancy (Yang et al., 2006) severely impairs mammary epithelial development in mice. In contrast, activation of PPAR β is accompanied by accelerated growth of mammary epithelium (our unpublished observation). Interestingly, evaluation of pertinent chromatin immunoprecipitation followed by deep sequencing (ChIP-seq) data from the Gene Expression Omnibus (GEO) repository (Yamaji et al., 2013; Lain et al., 2013; Kang et al., 2014) revealed that STAT5 and progesterone receptor (PR) bind strongly to promoter/enhancer regions of *Pxmp2* gene. Both, STAT5 and PR are known as major controlling transcriptional factors governing mammary gland development (Barash, 2006; Obr and Edwards, 2012; Obr et al., 2013).

According to our lipidomics data, the metabolism of fatty acids is compromised in the *Pxmp2*-deficient mammary fat pad. This is evident from the significant decrease in the content of myristic acid that may indicate deficiency in the export of the β -oxidation products from peroxisomes due to deletion of the *Pxmp2* channel (Antononkov and Hiltunen, 2012). We also found a decreased content of a set of diacylglycerols and phospholipids containing mostly polyunsaturated fatty acids in the fat pad of *Pxmp2*^{-/-} mice relative to wild-type animals. These results are in contrast to those generally observed on other models of peroxisomal disorders that display an elevation in the concentrations of very long-chain fatty acids, branched chain fatty acids, and bile acid precursors as well as a decrease in the content of plasmalogenes (Baes and Van Veldhoven, 2012). These data were mostly collected using models of generalized malfunctioning of peroxisomes. However, mice deficient in specific peroxisomal proteins frequently show a phenotype with tissue preference including local disturbances in lipid metabolism (Baes and Van Veldhoven, 2012, Fransen et al., 2012). These later observations are in accordance with the phenotype of *Pxmp2*^{-/-} mice since we did not find any abnormalities in lipid composition in the body fluids but only in the mammary fat pad of transgenic animals.

The mechanistic link between the *Pxmp2*-dependent lipid metabolism in the mammary fat pad and the defective mammary epithelial growth remains to be established. Our data did not reveal the involvement of oxidative stress and lipid peroxidation as factors connecting these processes. Instead, our observations indicating that the *Pxmp2* deficiency in mammary stroma affects growth of epithelium point to the potential role of regulatory factors involved in the cross-talk between these two compartments. This coincides with our finding that *Pxmp2* deficiency has an effect on the expression pattern of peroxisomal proteins in mammary fat pad. All these data indicate that in addition to a direct effect on lipid metabolism, *Pxmp2* deficiency may affect the regulatory pathways coordinated by lipid-sensing proteins. This prediction is in accordance with the data showing that deletion of peroxisomal multifunctional protein 2 involved in β -oxidation resulted in coordinate induction of PPAR α and SREBP2 (Martens et al., 2008). Even mild metabolic disturbances in stromal cells caused by *Pxmp2* deletion would affect mechanisms governing epithelial cell proliferation through activation or suppression of different receptors or other proteins by compounds produced in peroxisomes. For instance, deficiency in myristic acid may delay myristoylation of proteins involved in regulation of mammary epithelium development, such as members of the Wnt- β -catenin pathway (Jarde and Dale, 2012; Hu et al., 2010) while a decrease in the content of polyunsaturated fatty acids in phospholipids would affect lipid composition of biological membranes, which is an important factor in cell growth and differentiation (Sampaio et al., 2011).

In conclusion, here we reveal that the peroxisomal membrane channel protein, *Pxmp2*, is essential for the promotion of mammary gland development in mice. We also describe the key role of the mammary stroma in the *Pxmp2*-dependent epithelial growth and find that deletion of the *Pxmp2* gene results in abnormal lipid homeostasis in the mammary fat pad. The *Pxmp2*^{-/-} mouse model represents a novel and useful tool for investigation of lipid metabolism as well as lipid-sensitive signaling between mammary fat pad and epithelium, which are of value in understanding mechanisms of mammary gland development.

Acknowledgements

This work was supported by grants from the Academy of Finland, Sigrid Juselius Foundation and Orion-Farmos Research Foundation. The authors would like to thank Leena Ollitero,

Remya R. Nair, and Daniela Mennerich for technical assistance and members of ZORA biosciences staff: Kim Ekroos and Laura Heiskanen for analysis of complex lipids.

Appendix A. Supporting information

Supplementary data associated with this article can be found in the online version at <http://dx.doi.org/10.1016/j.ydbio.2014.03.022>.

References

- Ahle Meyer, B., Gottwald, M., Baumgart-Vogt, E., 2012. Deletion of a single allele of the *Pex11 β* gene is sufficient to cause oxidative stress, delayed differentiation and neuronal death in mouse brain. *Dis. Model. Mech.* 5, 1–16.
- Antononkov, V.D., Hiltunen, J.K., 2012. Transfer of metabolites across the peroxisomal membrane. *Biochim. Biophys. Acta* 1822, 1374–1386.
- Antononkov, V.D., Grunau, S., Ohlmeier, S., Hiltunen, J.K., 2010. Peroxisomes are oxidative organelles. *Antioxid. Redox Signal.* 13, 525–537.
- Antononkov, V.D., Sormunen, R.T., Hiltunen, J.K., 2004. The behavior of peroxisomes *in vitro*: mammalian peroxisomes are osmotically sensitive particles. *Am. J. Physiol. Cell Physiol.* 287, C1623–C1635.
- Baes, M., Van Veldhoven, P.P., 2012. Mouse models for peroxisome biogenesis defects and β -oxidation enzyme deficiencies. *Biochim. Biophys. Acta* 1822, 1489–1500.
- Barash, I., 2006. Stat5 in the mammary gland: controlling normal development and cancer. *J. Cell. Physiol.* 209, 305–313.
- Berryhill, G.E., Gloviczki, J.M., Trott, J.F., Aimo, L., Kraft, J., Cardiff, R.D., Paul, C.T., Petrie, W.K., Lock, A.L., Hovey, R.C., 2012. Diet-induced metabolic change induces estrogen-independent allometric mammary growth. *Proc. Nat. Acad. Sci. U.S.A.* 109, 16294–16299.
- Bottelbergs, A., Verheijden, S., Hulshagen, L., Gutmann, D.H., Goebbels, S., Nave, K.-A., Kassmann, C., Baes, M., 2010. Axonal integrity in the absence of functional peroxisomes from projection neurons and astrocytes. *Glia* 58, 1532–1543.
- Brisken, C., 2013. Progesterone signaling in breast cancer: a neglected hormone coming into the limelight. *Nat. Rev. Cancer* 13, 385–396.
- Brisken, C., Park, S., Vass, T., Lydon, J.P., O'Malley, B.W., Weinberg, R.A., 1998. A paracrine role for the epithelial progesterone receptor in mammary gland development. *Proc. Nat. Acad. Sci. U.S.A.* 95, 5076–5081.
- Cases, S., Zhou, P., Shillingford, J.M., Wiseman, B.S., Fish, J.D., Angle, C.S., Henningshausen, L., Werb, Z., Farese, R.V., 2004. Development of the mammary gland requires DGAT1 expression in stromal and epithelial tissues. *Development* 131, 3047–3055.
- Ciarloni, L., Mallepell, S., Brisken, C., 2007. Amphiregulin is an essential mediator of estrogen receptor alpha function in mammary gland development. *Proc. Nat. Acad. Sci. U.S.A.* 104, 5455–5460.
- Chevillard, G., Clemencet, M.C., Latruffe, N., Nicolas-Frances, V., 2004. Targeted disruption of the peroxisomal thiolase B gene in mouse: a new model to study disorders related to peroxisomal metabolism. *Biochemie* 86, 849–856.
- Cohen, P.E., Zhu, L., Nishimura, K., Pollard, J.W., 2002. Colony-stimulating factor 1 regulation of neuroendocrine pathways that control gonadal function in mice. *Endocrinology* 143, 1413–1422.
- Ekroos, K., 2008. Unraveling glycerophospholipidomes by lipidomics. In: Wan, F. (Ed.), *In: Biomarker Methods in Drug Discovery and Development*, (Ed.) Humana Press, pp. 369–384.
- Ekroos, K., Ejsing, C.S., Bahr, U., Karas, M., Simons, K., Shevchenko, A., 2003. Charting molecular composition of phosphatidylcholines by fatty acid scanning and ion trap MS3 fragmentation. *J. Lipid Res.* 44, 2181–2192.
- Fernandes, C.G., Leipnitz, G., Seminotti, B., Amaral, A.U., Zanatta, A., Vargas, C.R., Dutra Filho, D.S., Wajner, M., 2010. Experimental evidence that phenylalanine provokes oxidative stress in hippocampus and cerebral cortex of developing rats. *Cell. Mol. Neurobiol.* 30, 317–326.
- Flint, D.J., Travers, M.T., Barber, M.C., Binart, N., Kelly, P.A., 2005. Diet-induced obesity impairs mammary development and lactogenesis in murine mammary gland. *Am. J. Physiol.* 288, 1179–1187.
- Fransen, M., Nordgren, M., Bo, W., Apanasetis, O., 2012. Role of peroxisomes in ROS/RNS-metabolism: implications for human disease. *Biochim. Biophys. Acta* 1822, 1363–1373.
- Gouon-Evans, V., Rothenberg, M.E., Pollard, J.W., 2000. Postnatal mammary gland development requires macrophages and eosinophils. *Development* 127, 2269–2282.
- Hand, A.R., 1973. Morphologic and cytochemical identification of peroxisomes in the rat parotid and other exocrine glands. *J. Histochem. Cytochem.* 21, 131–141.
- Hovey, R.C., Aimo, L., 2010. Diverse and active roles for adipocytes during mammary gland growth and function. *J. Mammary Gland Biol. Neoplasia* 15, 279–290.
- Howlin, J., McBryan, J., Martin, F., 2006. Pubertal mammary gland development: insights from mouse models. *J. Mammary Gland Biol. Neoplasia* 11, 283–297.
- Hu, T., Li, C., Cao, Z., Van Raay, T.J., Smith, J.G., Willert, K., Solnica-Krezel, L., Coffey, R. J., 2010. Myristoylated Naked2 antagonized Wnt- β -catenin activity by degrading dishevelled-1 at the plasma membrane. *J. Biol. Chem.* 285, 13561–13568.
- Jarde, T., Dale, T., 2012. Wnt signaling in murine postnatal mammary gland development. *Acta Physiol.* 204, 118–127.

- Jung, H.R., Sylvanne, T., Koistinen, K.M., Tarasov, K., Kauhanen, K.M., Ekroos, K., 2011. High throughput quantitative molecular lipidomics. *Biochim. Biophys. Acta* 1811, 925–934.
- Kang, K., Yamaji, D., Yoo, K.H., Robinson, G.W., Hennighausen, L., 2014. Mammary-specific gene activation of Stat5 during pregnancy and the establishment of H3K4me3 marks. *Mol. Cell. Biol.* 34, 464–473.
- Kassmann, C.M., Lappe-Siefke, C., Baes, M., Brugger, B., Mildner, A., Werner, H.B., Natt, O., Michaels, T., Prinz, M., Frahm, J., Nave, K.-A., 2007. Axonal loss and neuroinflammation caused by peroxisome-deficient oligodendrocytes. *Nat. Genet.* 39, 969–976.
- Lain, A.R., Creighton, C.J., Conneely, O.M., 2013. Research resource: progesterone receptor targetome underlying mammary gland branching morphogenesis. *Mol. Endocrinol.* 27, 1743–1761.
- Landskroner-Eiger, S., Park, J., Israel, D., Pollard, J.W., Scherer, P.E., 2010. Morphogenesis of the developing mammary gland: stage-dependent impact of adipocytes. *Dev. Biol.* 344, 968–978.
- Lanigan, F., O'Connor, D., Martin, F., Gallagher, W.M., 2007. Molecular links between mammary gland development and breast cancer. *Cell. Mol. Life Sci.* 64, 3159–3184.
- Lee, S.S., Pineau, T., Drago, J., Lee, E.G., Owens, J.W., Kroetz, D.L., Fernandez-Salguero, P.M., Westphal, H., Gonzales, F.G., 1995. Targeted disruption of the alpha isoform of the peroxisome proliferator-activated receptor gene in mice results in abolishment of the pleiotropic effects of peroxisome proliferators. *Mol. Cell. Biol.* 15, 3012–3022.
- Lopez-Erauskin, L., Fourcade, S., Galino, J., Ruiz, M., Schluter, A., Naudi, A., Jove, M., Portero-Otin, M., Pamplona, R., Ferrer, I., Pujol, A., 2011. Antioxidants halt axonal degeneration in a mouse model of X-adrenoleukodystrophy. *Ann. Neurol.* 70, 84–92.
- Mallepell, S., Krust, A., Chambon, P., Briskin, C., 2006. Paracrine signaling through the epithelial estrogen receptor α is required for proliferation and morphogenesis in the mammary gland. *Proc. Nat. Acad. Sci. U.S.A.* 103, 2196–2201.
- Martens, K., Ver Loren van Themaat, E., van Batenburg, M.F., Heinäniemi, M., Huyghe, S., Van Hummelen, P., Calberg, C., Van Veldhoven, P.P., Van Kampen, A., Baes, M., 2008. Coordinate induction of PPAR α and SREBP2 in multifunctional protein 2 deficient mice. *Biochim. Biophys. Acta* 1781, 694–702.
- McCready, J., Arendt, L.M., Rudnick, J.A., Kuperwasser, C., 2010. The contribution of dynamic stromal remodeling during mammary development to breast carcinogenesis. *Breast Cancer Res.* 12, 205–214.
- McNally, S., Martin, F., 2011. Molecular regulators of pubertal mammary gland development. *Ann. Med.* 43, 212–234.
- Moinard, C., Cynober, L., de Bandt, J.P., 2005. Polyamines: metabolism and implications in human diseases. *Clin. Nutr.* 24, 184–197.
- Neville, M.C., McFadden, T.B., Forsyth, I., 2002. Hormonal regulation of mammary differentiation and milk secretion. *J. Mammary Gland Biol. Neoplasia* 7, 49–66.
- Obr, A.E., Edwards, D.P., 2012. The biology of progesterone receptor in the normal mammary gland and in breast cancer. *Mol. Cell. Endocrinol.* 357, 4–17.
- Obr, A.E., Grimm, S.L., Bishop, K.A., Pike, J.W., Lydon, J.P., Edwards, D.P., 2013. Progesterone receptor and Stat5 signalling cross talk through RANKL in mammary epithelial cells. *Mol. Endocrinol.* 27, 1808–1824.
- Olson, L.K., Tan, Y., Zhao, Y., Aupperlee, M.D., Haslam, S.Z., 2010. Pubertal exposure of high fat diet causes mouse strain-dependent alterations in mammary gland development and estrogen responsiveness. *Int. J. Obes.* 34, 1415–1426.
- Pirinen, E., Kuulasmaa, T., Pietilä, M., Heikkinen, S., Tusa, M., Itkonen, P., Boman, S., Skommer, J., Virkamäki, A., Hohtola, E., Kettunen, M., Fatrai, S., Kansanen, E., 2007. Enhanced polyamine catabolism alters homeostatic control of white adipose tissue mass, energy expenditure, and glucose metabolism. *Mol. Cell. Biol.* 27, 4953–4967.
- Qi, C., Zhu, Y., Pan, J., Usuda, N., Maeda, N., Yeldandi, A.V., Rao, M.S., Hashimoto, T., Reddy, J.K., 1999. Absence of spontaneous peroxisome proliferation in enoyl-CoA hydratase/L-3-hydroxyacyl-CoA dehydrogenase-deficient mouse liver. *J. Biol. Chem.* 274, 15775–15780.
- Reddy, J.K., Hashimoto, T., 2001. Peroxisomal β -oxidation and peroxisome proliferator activated receptor α : an adaptive metabolic system. *Annu. Rev. Nutr.* 21, 193–230.
- Robinson, G.W., Hennighausen, L., 1997. Inhibins and activins regulate mammary epithelial cell differentiation through mesenchymal-epithelial interactions. *Development* 124, 2701–2708.
- Rokka, A., Antonenkov, V.D., Soininen, R., Immonen, H.L., Pirilä, P.L., Bergmann, U., Sormunen, R.T., Weckstrom, M., Benz, R., Hiltunen, J.K., 2009. Pxm2 is a channel-forming protein in mammalian peroxisomal membrane. *PLoS One* 4, e5090.
- Sampaio, J.L., Gerl, M.J., Klose, C., Ejsing, C.S., Beug, H., Simons, K., Shevchenko, A., 2011. *Proc. Nat. Acad. Sci.* 108, 1903–1907.
- Savolainen, K., Kotti, T.J., Schmitz, W., Savolainen, T.I., Sormunen, R.T., Ilves, M., Vainio, S.J., Conzelmann, E., Hiltunen, J.K., 2004. A mouse model for alpha-methylacyl-CoA racemase deficiency: adjustment of bile acid synthesis and intolerance to dietary methyl-branched lipids. *Hum. Mol. Gen.* 13, 955–965.
- Schupp, M., Lazar, M.A., 2010. Endogenous ligands for nuclear receptors: digging deeper. *J. Biol. Chem.* 285, 40409–40415.
- Singh, I., Pujol, A., 2010. Pathomechanisms underlying X-adrenoleukodystrophy: a three-hit hypothesis. *Brain Pathol.* 20, 838–844.
- Sternlicht, M.D., Sunnarborg, S.W., 2008. The ADAM17-amphiregulin-EGFR axis in mammary development and cancer. *J. Mammary Gland Biol. Neoplasia* 13, 181–194.
- Tyurina, Y.Y., Tyurin, V.A., Epperly, M.W., Greenberger, J.S., Kagan, 2008. Oxidative lipidomics of γ -irradiation-induced intestinal injury. *Free Radical Biol. Med.* 44, 299–314.
- Wanders, R.J., Waterham, H.R., 2006. Biochemistry of mammalian peroxisomes revisited. *Annu. Rev. Biochem.* 75, 295–332.
- Wiesen, J.F., Young, P., Werb, Z., Cunha, G.R., 1999. Signaling through the stromal epidermal growth factor receptor is necessary for mammary ductal development. *Development* 126, 335–344.
- Wu, T., Yankovskaya, V., McIntire, W.S., 2003. Cloning, sequencing, and heterologous expression of the murine peroxisomal flavoprotein, N1-acetylated polyamine oxidase. *J. Biol. Chem.* 278, 20514–20525.
- Yamaji, D., Kang, K., Robinson, G.W., Hennighausen, L., 2013. Sequential activation of genetic programs in mouse mammary epithelium during pregnancy depends on STAT5A/B concentration. *Nucleic Acids Res.* 41, 1622–1636.
- Yang, Q., Kurotani, R., Yamada, A., Kimura, S., Gonzalez, F.G., 2006. Peroxisome proliferator-activated receptor α activation during pregnancy severely impairs mammary lobuloalveolar development in mice. *Endocrinology* 147, 4772–4780.